

Supporting Information

Stable and Efficient Solar-Driven Photoelectrochemical Water Splitting into H₂ and O₂ Based on BaTaO₂N Photoanode Decorated with CoO Microflowers

Shunhang Wei, ‡^a Shufang Chang, ‡^a Fan Yang,^b Zhengping Fu,^c Gang Liu^{d,e}
and Xiaoxiang Xu*^a

^aPutuo People's Hospital, Shanghai Key Lab of Chemical Assessment and Sustainability, School of Chemical Science and Engineering, Tongji University, Shanghai, 200060, China.

^bNew Energy Automotive Center, School of Automotive Studies, Tongji University, Shanghai, 201804, China.

^cDepartment of Materials Science and Engineering, CAS Key Laboratory of Materials for Energy Degradation, University of Science and Technology of China, Hefei, 230026, China

^dShenyang National laboratory for Materials Science, Institute of Metal Research, Chinese Academy of Science, 72 Wenhua Road, Shenyang, 110016, China

^eSchool of Materials Science and Engineering, University of Science and Technology of China, 72 Wenhua Road, Shenyang 110016, China

*Corresponding author

Xiaoxiang Xu (Email: xxxu@tongji.edu.cn; Tel: +86-021-65986919)

‡These authors contribute equally.

Supporting information content

Number of pages: 22 (S1-S22)

Number of figures: 12 (Figure S1-S12)

Number of tables: 1 (Table S1)

Content

Experimental details **S5-S9**

Figure S1 X-ray powder diffraction (XRD) patterns of bare CoO, bare BaTaO₂N and CoO@ BaTaO₂N photoanode, standard patterns for CoO, BaTaO₂N and FTO are also included. **S10**

Figure S2 FESEM images of BaTaO₂N: (a) cross-section view and (b) top view; FESEM images of CoO@BaTaO₂N: (c) cross-section view and (d) top view **S11**

Figure S3 (a) TEM image of BaTaO₂N; (b) selected area electron dispersive X-ray spectroscopy (EDS) analysis at marked area of (a), cation compositions are listed in the table inserted, standard deviations are included in the parenthesis. **S12**

Figure S4 TEM image of CoO@BaTaO₂N after sonication treatment **S13**

Figure S5 UV-vis absorption spectra of CoO, BaTaO₂N and CoO@ BaTaO₂N **S14**

Figure S6 X-ray absorption spectra (XAS) of CoO microflowers, spectra of CoO and Co₂O₃ standard are also shown for comparisons. Linear combination fitting based on the reference spectra suggests a Co²⁺/Co³⁺ ratio around 2/3. **S15**

Figure S7 Figure S7. Linear sweep voltammetry of bare BaTaO₂N photoanode, CoO@BaTaO₂N photoanode and Co-Pi@ BaTaO₂N photoanode under chopped visible light illumination ($\lambda \geq 420$ nm) **S16**

Figure S8 Linear sweep voltammetry of BaTaO₂N photoelectrode deposited with CoO microflowers and CoO nanoparticles under chopped visible light illumination ($\lambda \geq 420$ nm) **S17**

Figure S9 FESEM image of CoO@BaTaO₂N photoelectrode after long tem PEC analysis **S18**

Figure S10 (a) Solar irradiance of AM 1.5 and integrated absorption photocurrent of BaTaO₂N and CoO@BaTaO₂N. The integrated absorption photocurrent is obtained by multiplying the AM 1.5 solar spectrum with the absorption spectrum; (b) dark current (dotted line) and photocurrent under AM 1.5 illumination (solid line) of BaTaO₂N with and without Na₂SO₃ (0.05 M) in KOH aqueous solution (0.1 M, pH = 13); (c) dark current (dotted line) and photocurrent under AM 1.5 illumination (solid line) of CoO@BaTaO₂N with and without Na₂SO₃ (0.05 M) in KOH aqueous solution (0.1 M, pH = 13)

S19

Figure S11 Surface charge transfer efficiency of bare BaTaO₂N and CoO@ BaTaO₂N. **S20**

Figure S12 Mott-Schottky (MS) analysis of (a) BaTaO₂N and (b) CoO; their flat band potential can be determined by extrapolating the linear part of MS curves down to the potential axis. BaTaO₂N is a typical n-type semiconductor whilst CoO is p-type one according to the positive and negative MS curve slop, respectively. Assuming a 0.2 eV difference between flat band potential and conduction (valence) band for BaTaO₂N (CoO), the band edge alignment of both compounds can be deduced.

S21

Table S1 Summary of fitted electron lifetime τ and their relative amplitude of

BaTaO₂N and CoO@BaTaO₂N deduced from the time-resolved PL spectra **S22**

Reference **S22**

Experimental

Synthesis of BaTaO₂N

BaTaO₂N samples were prepared according to previous report¹. In brief, stoichiometric amounts of BaNO₃ (SCR, 99.5%), TaCl₅ (Alfa Aesar, 99.99%) were dissolved in 10 ml ethylene glycol (Aladdin, 98%) containing 1.8 g anhydrous citric acid (Aladdin, 99.5%). Heating at 423 K and magnetic stirring was used to facilitate dissolution of all chemicals. The so-formed transparent solution was heated at 573 K which was gradually turned into brown resin due to polymerization. The resin was transferred into alumina crucible and calcined at 823 K for 10 h for the removal of organic species. The resultant white powders were transferred into a tube furnace for ammonolysis. Flowing ammonia gas (Jiaya Chemicals, 99.999%) was introduced into the tube furnace at a flowing rate of 250 ml min⁻¹. The furnace was then ramped to 1273 K, dwelled at 1273 K for 15 h and was cooled naturally to room temperature. The resultant red powders were analyzed by XRD for phase identification.

Photoelectrode preparation

Electrophoretic deposition method was adopted to prepare photoelectrodes²: two pieces of fluorine-doped tin oxide (FTO) glass (30 × 10 mm) were inserted in parallel into 50 ml acetone solution containing 70 mg BaTaO₂N powders and 10 mg iodine. 10 mm distance was kept for FTO glass with their conductive sides faced inward. Subsequently, a constant bias (10 V) was loaded for 3 min under a potentiostatic control (Keithley 2450Source Meter). BaTaO₂N powders were quickly deposited onto

FTO glass at the anode side which was then used as the photoelectrodes. These photoelectrodes were calcined in N₂ flow at 673 K for 1 h to remove absorbed iodine. TiCl₄ (Alfa Aesar, 99.99%) ethanol solution (10 mM) was dropped onto the photoelectrodes, and were dried at 623 K for 15 min. This treatment was repeated for six times in order to improve particle-interconnection and to reduce exposure of naked FTO. The photoelectrodes were then calcined in N₂ flow at 673 K for another 1 h.

***In situ* growth of CoO microflowers onto BaTaO₂N photoelectrodes**

CoO microflowers were *in situ* grown onto BaTaO₂N photoelectrodes by a hydrothermal method: Co(NO₃)₂·6H₂O (1 mmol) and urea (2 mmol) were dissolved into 30 ml deionized water as a precursor solution. Freshly prepared BaTaO₂N photoelectrodes were immersed into above solution, and were transferred into a Teflon-lined stainless steel autoclave for hydrothermal reactions. Typical reaction temperature is 393 K and reaction time is 5 h. After cooling the autoclave naturally, the photoelectrodes were taken out, and were rinsed by deionized water for a few times. The photoelectrodes were further calcined in N₂ flow at 673 K for 1 h, and was denoted as CoO@BaTaO₂N. For comparisons, CoO nanoparticles were also loaded onto BaTaO₂N using conventional impregnation method according to previous reports^{3, 4}. Cobalt phosphate (Co-Pi) was also loaded onto BaTaO₂N for comparisons according to previous report⁵.

Basic characterization

Phase compositions were analyzed by X-ray powder diffraction (XRD) techniques on a Bruker D8 Focus diffractometer. Incident radiation was Cu K α 1 ($\lambda = 1.5406 \text{ \AA}$) and Cu K α 2 ($\lambda = 1.5444 \text{ \AA}$). Diffuse reflectance spectra were collected using a UV-Vis spectrometer (JASCO-V750) and were analyzed using JASCO software suite. BaSO₄ was used as a non-absorbing reference material. The morphology of the samples was inspected under a field emission scanning electron microscope (Hitachi S4800, Japan) and a transmission electron microscope (JEOL JEM-2100, Japan). Photoluminescence spectra (PL) and time-resolved PL decay spectra were recorded using a spectrofluorometer (FLUOROLOG-3-11) with an excitation wavelength of 260 nm. The soft X-ray absorption spectra (XAS) were collected at the BL10B of the National Synchrotron Radiation Laboratory (NSRL, Hefei, P. R. China). X-ray photoelectron spectroscopy (XPS, AXIS Ultra DLD) technique was introduced to investigate the surface state of sample powders. A monochromatic Al K α X-ray was used as the radiation source. The spectra data was adjusted properly using adventitious C 1s state (284.8 eV)⁶.

Photoelectrochemical (PEC) measurements

PEC experiments were performed in a gas-tight PEC cell with a three-electrode configuration connected to a Zahner electrochemical workstation. The photoelectrode, Pt foil (10 \times 10 mm) and Ag/AgCl electrode were used as working, counter and reference electrodes, respectively. Potentials are recorded vs. reversible hydrogen electrode (RHE), which is obtained using the formula $E_{\text{RHE}} = E_{\text{Ag/AgCl}} + 0.059\text{pH} +$

0.1976 V. KOH aqueous solution (0.1 M, pH = 13) was used as an electrolyte. A 300 W Xenon lamp (PLX-SXE300, Perfect Light, China) coupled with a cut-off filter ($\lambda \geq 420$ nm or AM 1.5G) was applied as the light source. The solution was purged with Ar for 20 min prior to the PEC measurement. Incident light was rectified by an electronic timer and shutter (GCI-73 DAHENG, China). The wavelength dependent incident photon-to-current conversion efficiency (IPCE) was calculated according to the following equation:

$$\text{IPCE}(\%) = [1240 \times I_{\lambda}] / [\lambda \times P_{\text{Input}}] \times 100\%$$

where I_{λ} (mA cm⁻²) is the steady-state photocurrent density under monochromatic irradiation of wavelength λ , P_{input} (mW cm⁻²) is the incident photon density measured by a photometer. Tunable monochromatic irradiation was produced by combining a monochromator (TLS300XENON150, NBet, China) with a 300 W Xenon lamp (NBet, China). Gas composition within the PEC cell was analyzed by a gas chromatograph (GC7900 TECHCOMP, China) using Ar as a carrier gas and a TCD detector. Mott-Schottky (MS) analysis was performed using the same three-electrode configuration by analyzing the impedance spectra at 1000 Hz from -0.8 V to 1 V vs NHE. Capacitance was extracted from impedance data and used for MS plot.

Detection of photogenerated holes.

As a chemical probe for detection of hole location⁷, MnO₂ was photo-deposited onto

photoelectrodes from manganese (II) chloride aqueous solution (0.2g L^{-1}). A 300 W Xenon lamp (Perfect Light, PLX-SXE300) coupled with AM 1.5G filter was applied as the light source. The photoelectrode was irradiated for 20 min at a bias of 1.23 V vs RHE. After deposition, the photoelectrode was rinsed with deionized water and was dried at room temperature before microscopic analysis.

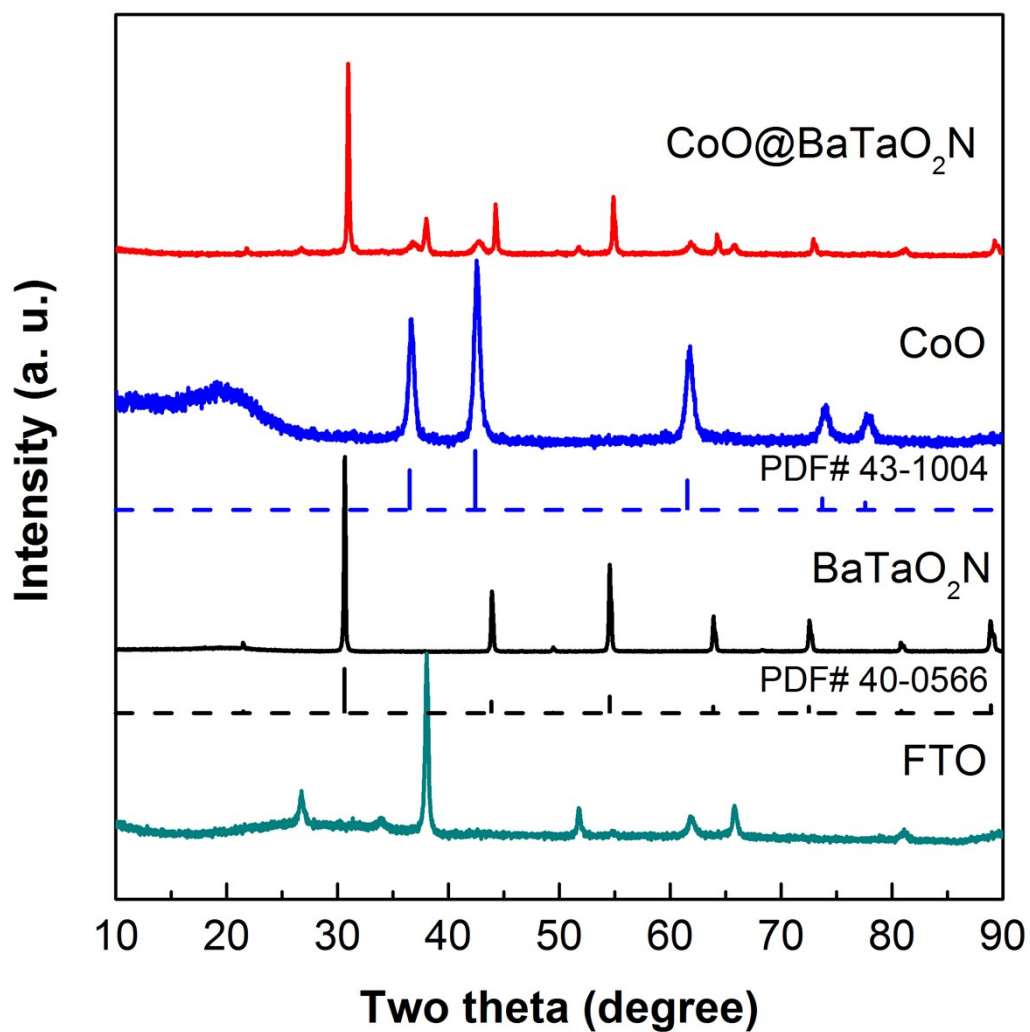


Figure S1. X-ray powder diffraction (XRD) patterns of bare CoO, bare BaTaO₂N and CoO@BaTaO₂N photoanode, standard patterns for CoO, BaTaO₂N and FTO are also included.

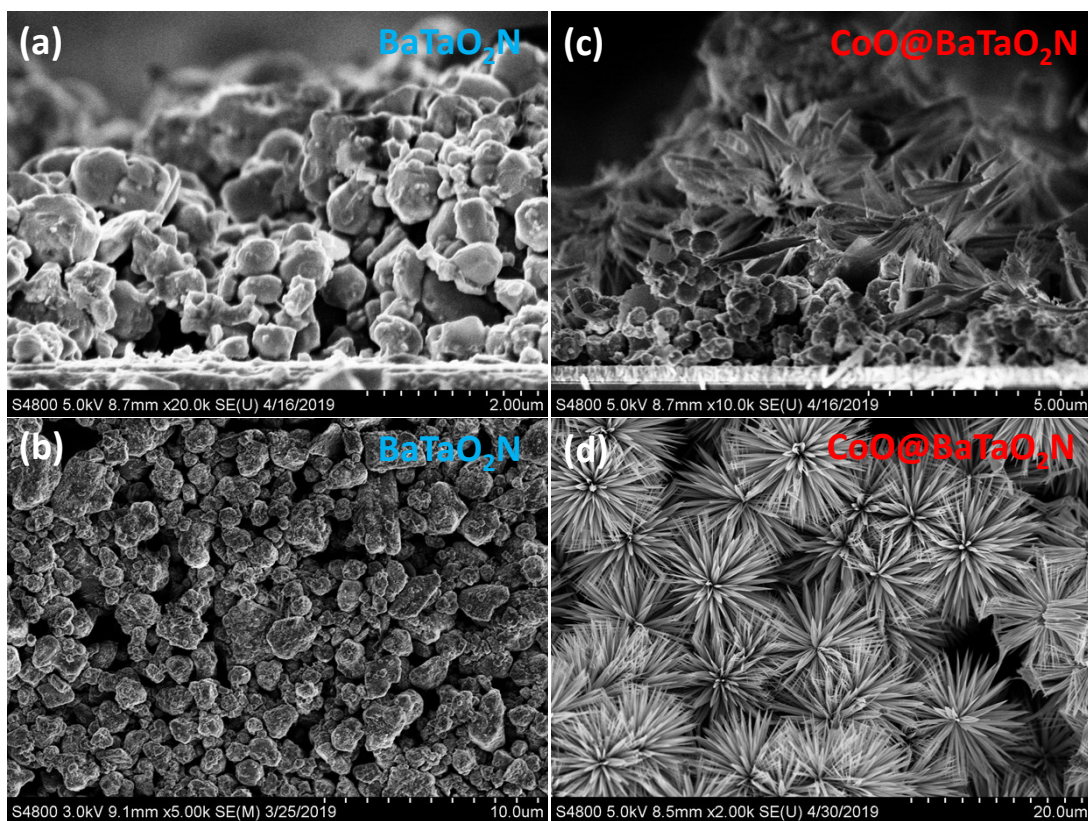


Figure S2. FESEM images of BaTaO₂N: (a) cross-section view and (b) top view; FESEM images of CoO@BaTaO₂N: (c) cross-section view and (d) top view

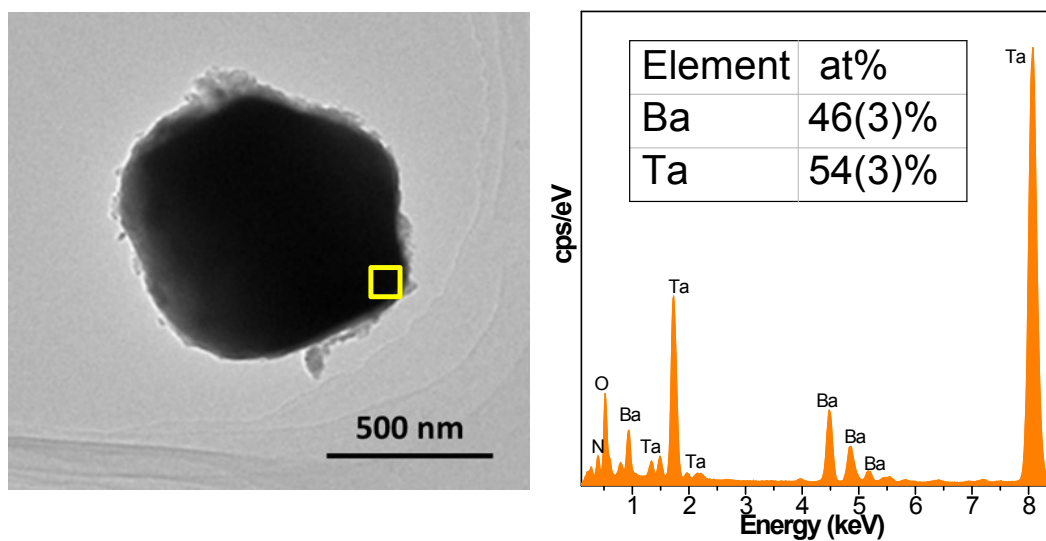


Figure S3. (a) TEM image of BaTaO₂N; (b) selected area electron dispersive X-ray spectroscopy (EDS) analysis at marked area of (a), cation compositions are listed in the table inserted, standard deviations are included in the parenthesis.

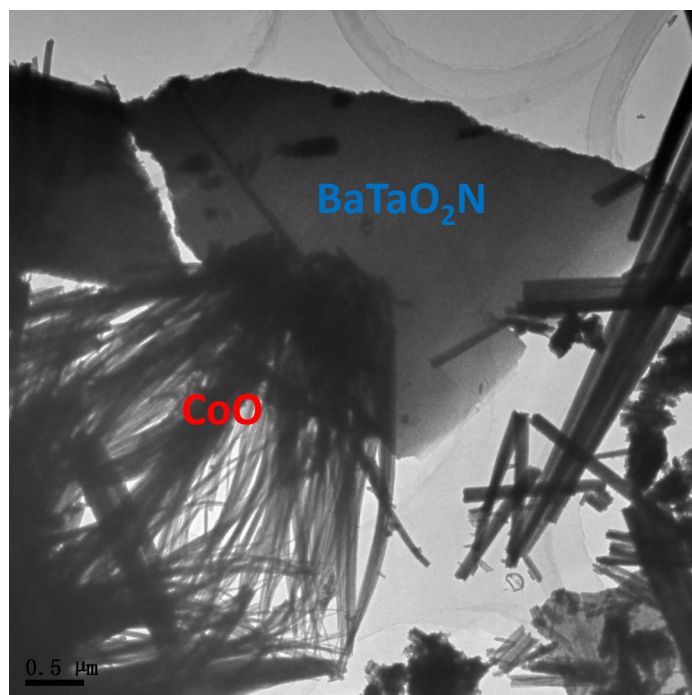


Figure S4. TEM image of CoO@BaTaO₂N after sonication treatment

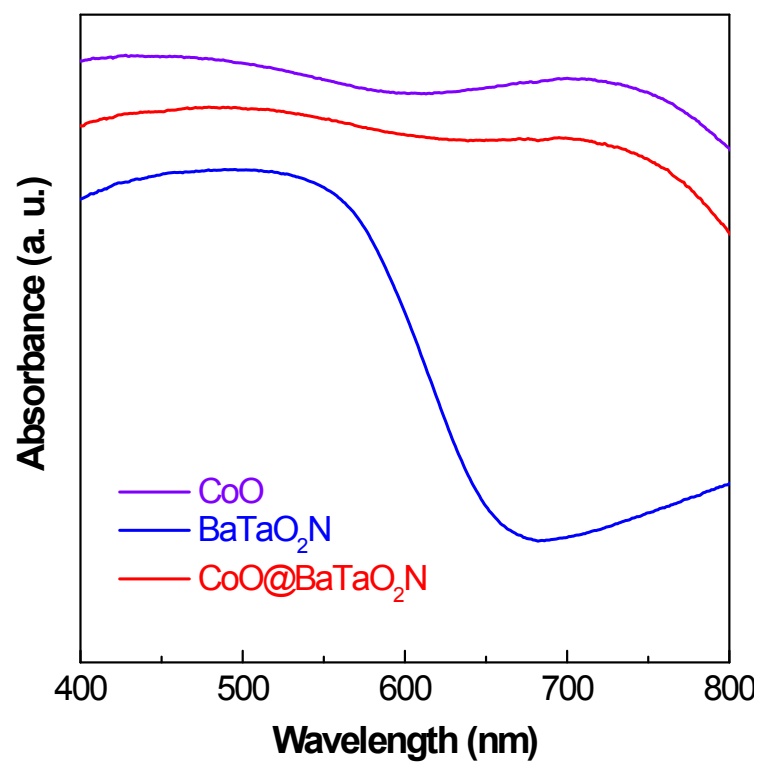


Figure S5. UV-vis absorption spectra of CoO, BaTaO₂N and CoO@BaTaO₂N

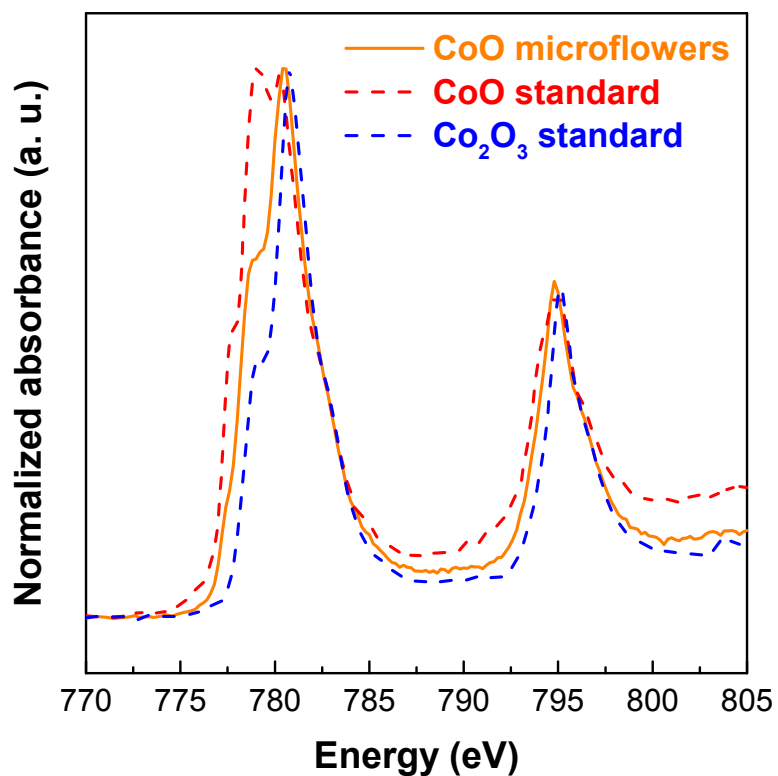


Figure S6. X-ray absorption spectra (XAS) of CoO microflowers, spectra of CoO and Co₂O₃ standard are also shown for comparisons. Linear combination fitting based on the reference spectra suggests a Co²⁺/Co³⁺ ratio around 2/3.

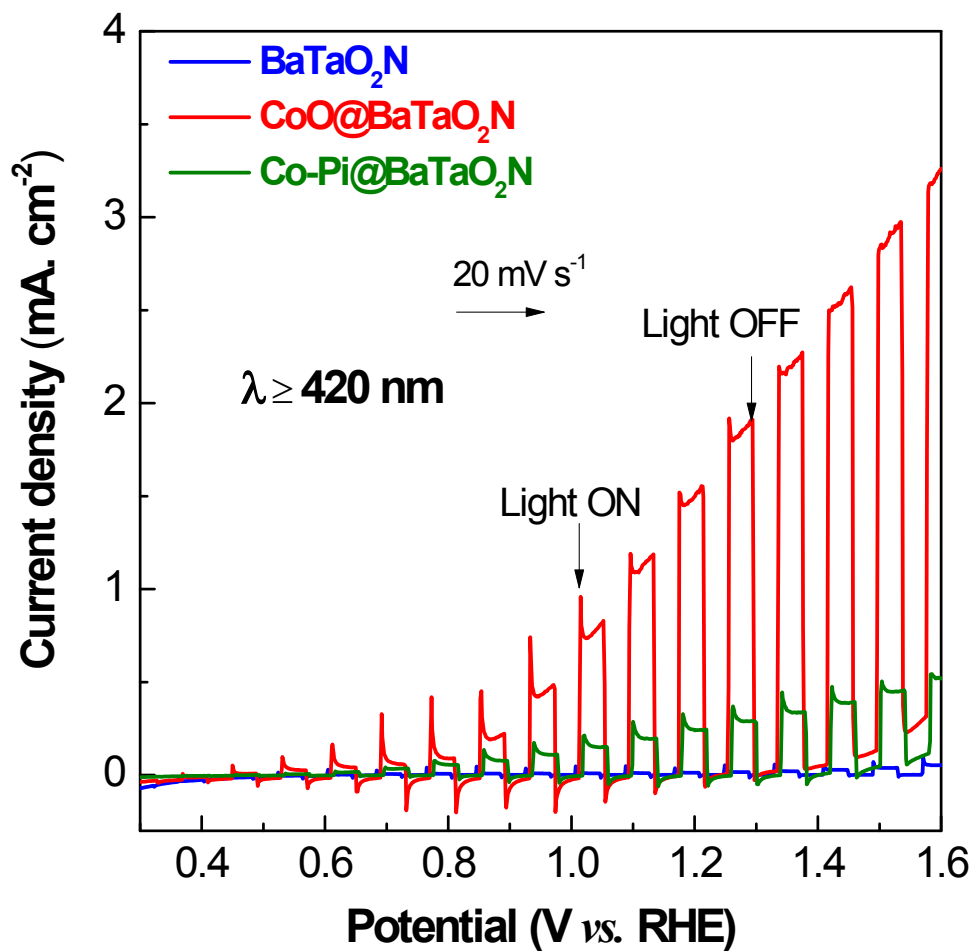


Figure S7. Linear sweep voltammetry of bare BaTaO₂N photoanode, CoO@BaTaO₂N photoanode and Co-Pi@ BaTaO₂N photoanode under chopped visible light illumination ($\lambda \geq 420$ nm)

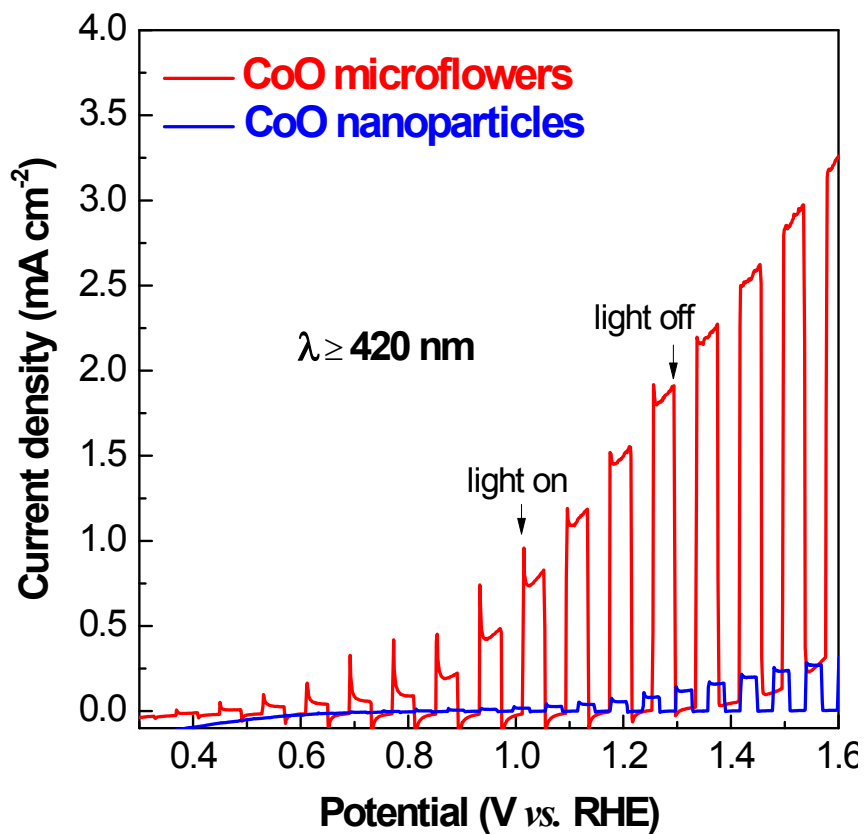


Figure S8. Linear sweep voltammetry of BaTaO₂N photoelectrode deposited with CoO microflowers and CoO nanoparticles under chopped visible light illumination ($\lambda \geq 420$ nm)

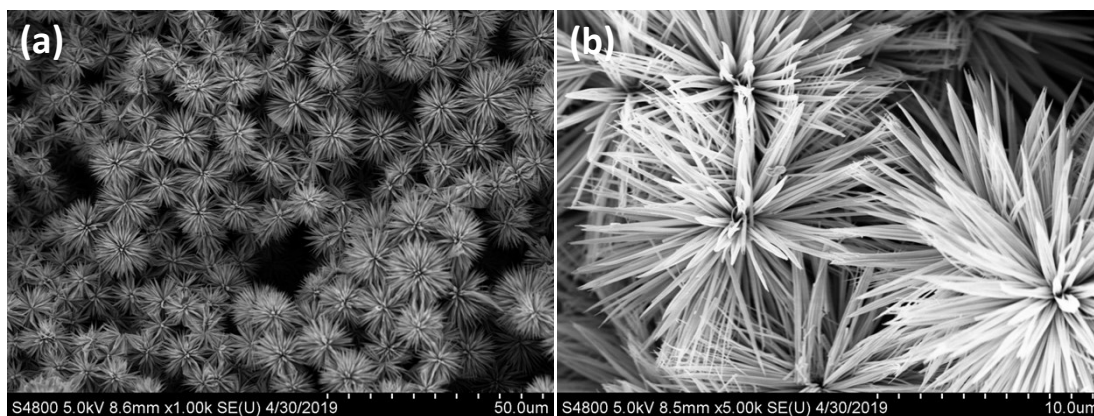


Figure S9. FESEM image of CoO@BaTaO₂N photoelectrode after long tem PEC analysis

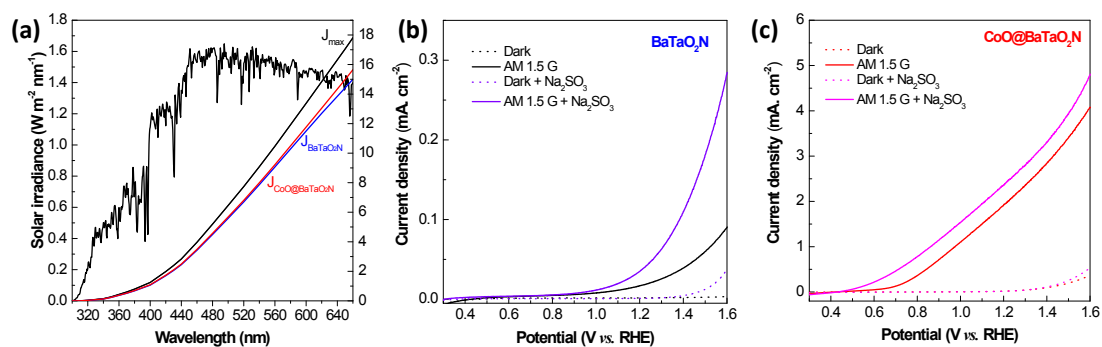


Figure S10. (a) Solar irradiance of AM 1.5 and integrated absorption photocurrent of BaTaO₂N and CoO@BaTaO₂N. The integrated absorption photocurrent is obtained by multiplying the AM 1.5 solar spectrum with the absorption spectrum; (b) dark current (dotted line) and photocurrent under AM 1.5 illumination (solid line) of BaTaO₂N with and without Na₂SO₃ (0.05 M) in KOH aqueous solution (0.1 M, pH = 13); (c) dark current (dotted line) and photocurrent under AM 1.5 illumination (solid line) of CoO@BaTaO₂N with and without Na₂SO₃ (0.05 M) in KOH aqueous solution (0.1 M, pH = 13)

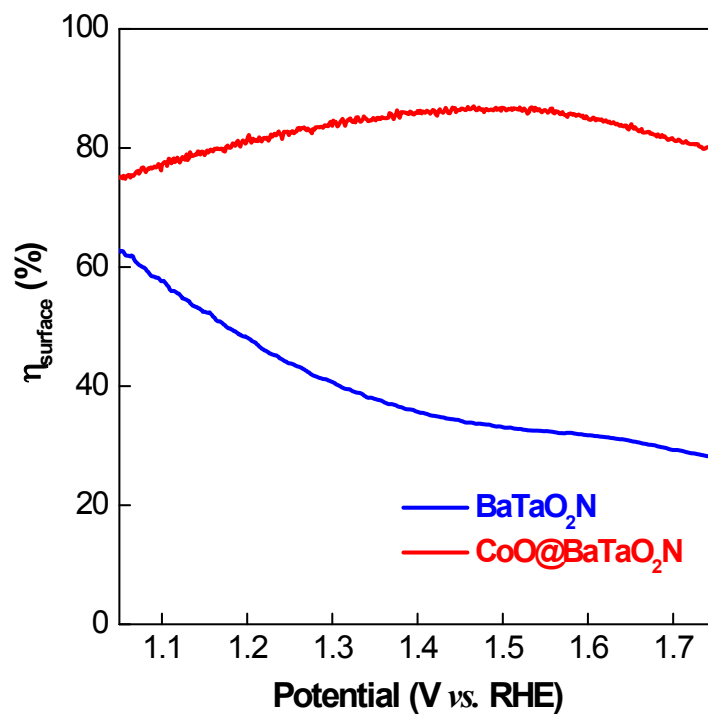


Figure S11. Surface charge transfer efficiency of bare BaTaO₂N and CoO@BaTaO₂N.

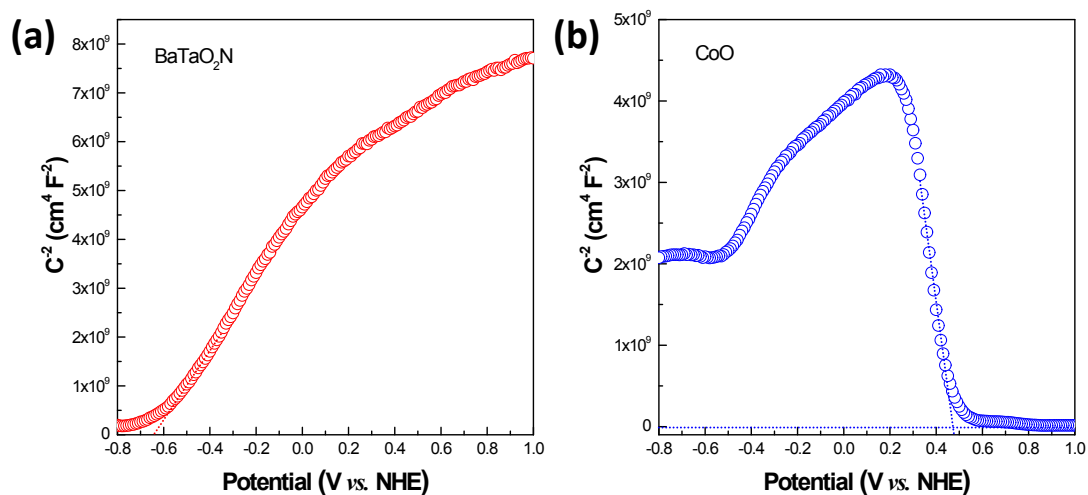


Figure S12. Mott-Schottky (MS) analysis of (a) BaTaO₂N and (b) CoO; their flat band potential can be determined by extrapolating the linear part of MS curves down to the potential axis. BaTaO₂N is a typical n-type semiconductor whilst CoO is p-type one according to the positive and negative MS curve slop, respectively. Assuming a 0.2 eV difference between flat band potential and conduction (valence) band for BaTaO₂N (CoO), the band edge alignment of both compounds can be deduced.

Table S1. Summary of fitted electron lifetime τ and their relative amplitude of BaTaO₂N and CoO@BaTaO₂N deduced from the time-resolved PL spectra

Sample	Fitted electron lifetime (ns)			Relative amplitude (%)			Average lifetime $\langle\tau\rangle$ (ns)	χ^2
	τ_1	τ_2	τ_3	f_1	f_2	f_3		
BaTaO ₂ N	22.2	189.9	1400.6	7.24	27.81	64.95	1332.0	1.02
CoO@BaTaO ₂ N	45.9	279.1	1790.7	7.86	27.89	64.26	1690.1	1.01

The average lifetime is calculated by equation:

$$\langle\tau\rangle = \frac{f_1\tau_1^2 + f_2\tau_2^2 + f_3\tau_3^2}{f_1\tau_1 + f_2\tau_2 + f_3\tau_3} \quad (S1)$$

χ^2 : the goodness of fit parameter.

Reference

1. H. Zhang, S. H. Wei and X. X. Xu, *J. Catal.*, 2020, **383**, 135-143.
2. Y. H. Xie, Y. W. Wang, Z. F. Chen and X. X. Xu, *ChemSusChem*, 2016, **9**, 1403-1412.
3. F. X. Zhang, A. Yamakata, K. Maeda, Y. Moriya, T. Takata, J. Kubota, K. Teshima, S. Oishi and K. Domen, *J. Am. Chem. Soc.*, 2012, **134**, 8348-8351.
4. S. H. Wei, G. Zhang and X. X. Xu, *Appl. Catal. B-Environ.*, 2018, **237**, 373-381.
5. S. K. Pilli, T. E. Furtak, L. D. Brown, T. G. Deutsch, J. A. Turner and A. M. Herring, *Energ. Environ. Sci.*, 2011, **4**, 5028-5034.
6. P. Van der Heide, *X-ray photoelectron Spectroscopy - An introduction to principles and practices*, John Wiley & Sons, Inc, Hoboken, New Jersey, 2012.
7. R. G. Li, F. X. Zhang, D. G. Wang, J. X. Yang, M. R. Li, J. Zhu, X. Zhou, H. X. Han and C. Li, *Nat. Commun.*, 2013, **4**, 1432.